ORIGINAL ARTICLE   **Open Access**

Deep Drawing Process Using a Tractrix Die for Manufacturing Liners for a CNG High-Pressure Vessel (Type II)

Gun-Young Park[1], Hyo-Seo Kwak[2], Hyo-Seong Jang[1] and Chul Kim[1*]

Abstract

The liner of a CNG pressure vessel is manufactured by a DDI (deep drawing and ironing) process for the cylinder part, which is a continuous process that includes a drawing process to reduce the diameter of the billet and a subsequent ironing process to reduce the thickness of the billet. A tractrix die used in the 1st deep drawing allows the blank to flow smoothly by decreasing the punch load and radial tensile stress occurring in the workpiece. It also increases the draw ratio compared to conventional dies, but it causes forming defects. In this study, a shape coefficient (S_c) is proposed for the tractrix die using the blank diameter (D_0), inflow diameter of the workpiece (d_i), and inflow angle of the workpiece (θ) for design of the tractrix die. The effects of the thickness and inflow angle of the workpiece on wrinkling and folding were investigated through FEA. Also, a discriminant is proposed for the relative radial stress ($\tilde{\sigma}$) generated during the deep drawing process using the tractirx die and used to predict fracture. Based on the results, the blank thickness, the draw ratio, and the inflow of the workpiece angle in the 1st deep drawing process are suggested, and the number of operations in the DDI process was reduced from 6 to 4. This improves the productivity and reduces the manufacturing cost.

Keywords: Tractrix die, Deep drawing, Wrinkling, Folding, LDR (Limit draw ratio), FEM

1 Introduction

The liner of a Type II CNG high-pressure vessel (34CrMo4) consists of a cylinder part obtained by DDI. DDI is a continuous process that includes deep drawing [1, 2] to reduce the billet diameter and ironing [3, 4] to decrease the thickness without change of the inner diameter. The manufacturing process for a liner obtained by spinning is composed of a 1st stage (deep drawing with a tractrix die), a 2nd stage (redrawing + ironing 1 + ironing 2), and a 3rd stage (redrawing + ironing), as shown in Figure 1 [5–7].

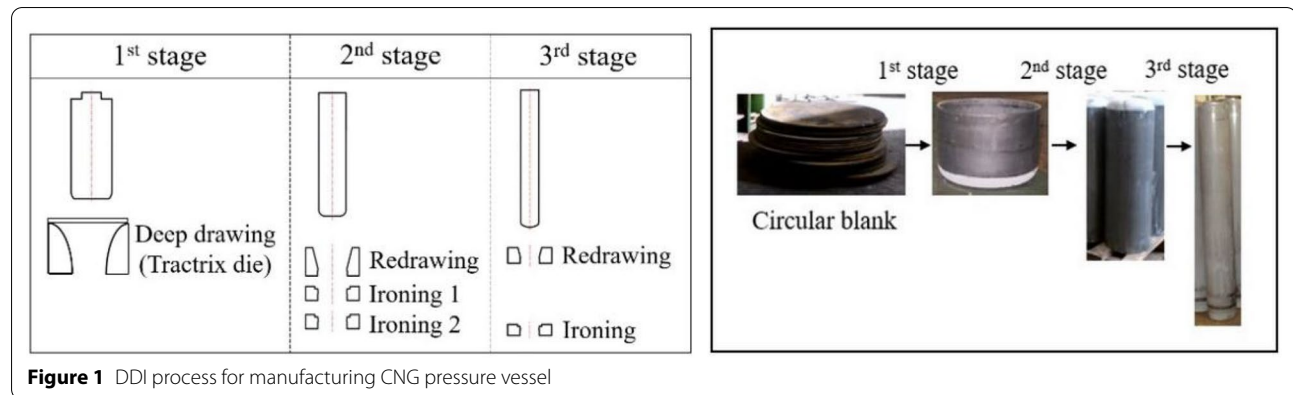Owing to the wrinkling and folding from compressive stress during the first deep drawing process [8, 9], using

a blank holder that forces the flange part of the sheet prevents from them [10–12]. But a CNG pressure vessel (Type II) is manufactured with a thick plate that has large resistance compared to a thin plate, so it is possible to form it by a simple tractrix die without a blank holder in a deep drawing process [13–15]. A simple tractrix die allows the blank to flow smoothly by decreasing the punch load and radial tensile stress applied to the blank wall, so it can increase the draw ratio compared to conventional dies [16], but care should be taken as forming defects may occur.

In a previous study on forming defects in a deep drawing process using a simple tractrix or conical die, Kesharwani designed a modified conical tractrix die to reduce the deformation force and to enhance the LDR (limit draw ratio). The formability of a tailor friction stir-welded sheet blank was improved by 27% [17]. Magrinho presented a new combined experimental and theoretical

*Correspondence: chulki@pusan.ac.kr
[1] School of Mechanical Engineering, Pusan National University, Pusan 46241, South Korea
Full list of author information is available at the end of the article

Park *et al. Chinese Journal of Mechanical Engineering*   (2022) 35:15

Page 2 of 12

Figure 1 DDI process for manufacturing CNG pressure vessel

methodology for determining the formability limits by wrinkling. They did this by using experimentation and finite element modeling of cylindrical deep-drawing without a blank holder combined with the space of the effective strain vs. stress [18].

Narayanasamy studied the wrinkling behavior of steels and their suitability for a drawing process with the help of experimental work using conical and simple tractrix dies under lubricated and non-lubricated conditions [19]. Abdullah proposed a simple process for deep drawing of elliptical cups without a blank holder and investigated the effect of the die and punch geometry according to the half-cone angle and punch fillet radius on the LDR and drawing load for the optimization of the process [20, 21]. Hezam developed a new process for increasing the drawability of square cups using a conical die with a square aperture at its end. The goal was to enable easy flow of the metal from the circular sections to the square aperture and the throat of the die [22].

The previous works have focused on a thin cylinder, and there is lack of study related to a thick blank. Forming defects in a deep drawing process using a tractrix die without a blank holder are associated with the initial
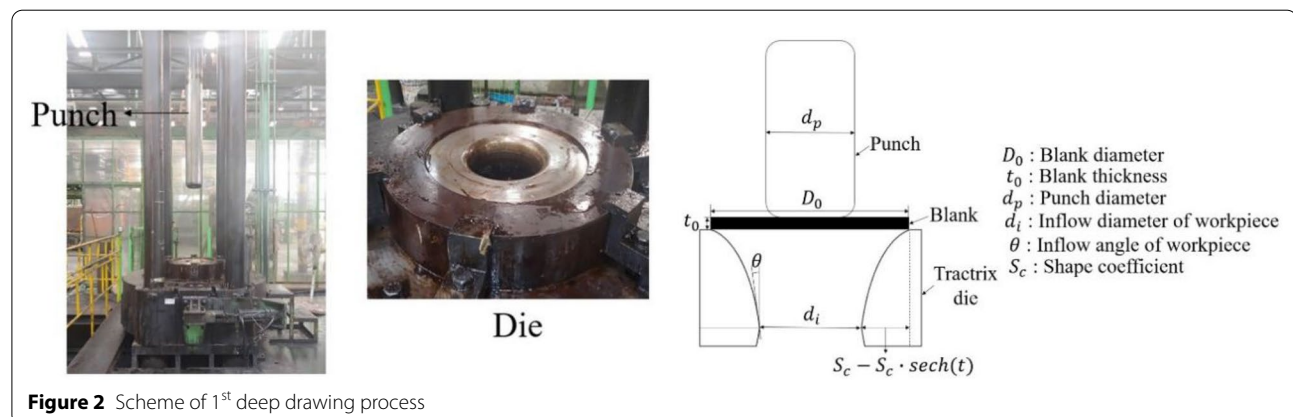
blank thickness and shape of the die [20–22]. In order to improve and optimize the current DDI process, a study on the relation between blank thickness and the shape of the tractrix die is needed.
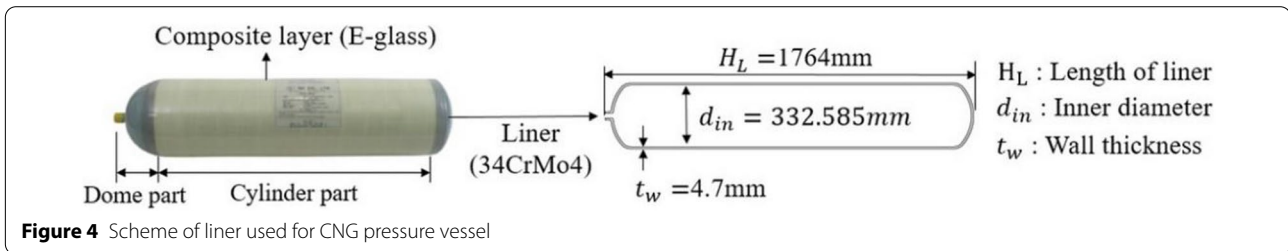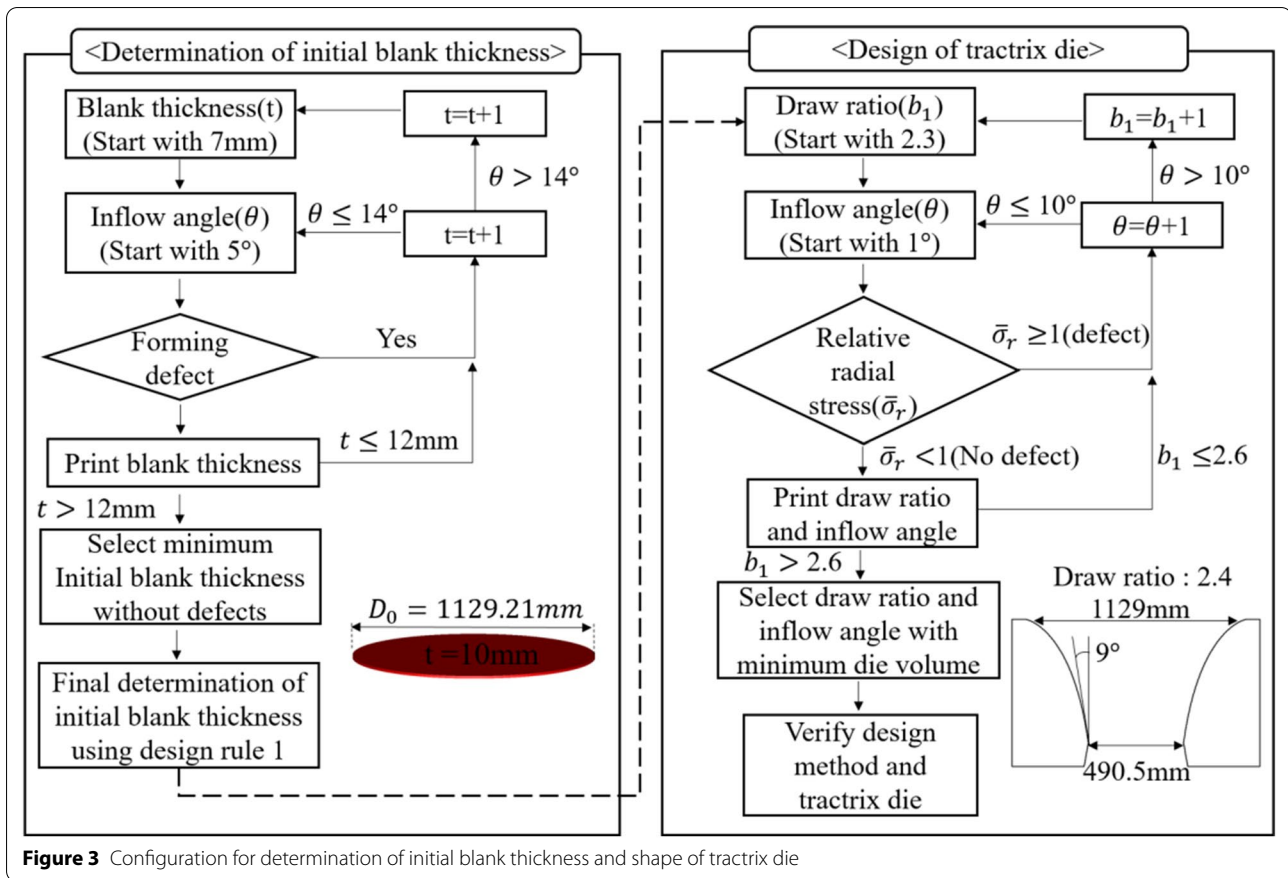
This study proposes a shape coefficient (S_C) for a tractrix die using the blank diameter (D_0), inflow diameter of the workpiece (d_i), and inflow angle of the workpiece (θ) for the design of a tractrix die, as shown in Figure 2. Effects of the thickness and inflow angle on wrinkling and folding were investigated through FEA. Also, a discriminant is proposed for the relative radial stress ($\bar{\sigma}_r$) generated during the deep drawing process using the tractrix die, and it was used to predict fracture. Based on the results, the minimum blank thickness, draw ratio, and inflow angle of the workpiece without forming defects are suggested. And flow chart of this study is shown in Figure 3.

2 Design of DDI Process to Manufacture Liner of Pressure Vessel

2.1 Design Rules of DDI Process in the Actual Field
Figure 4 illustrates the geometric details of the liner of a CNG high-pressure vessel, and Table 1 shows the design

Figure 2 Scheme of 1st deep drawing process

Figure 3 Configuration for determination of initial blank thickness and shape of tractrix die

Figure 4 Scheme of liner used for CNG pressure vessel

Table 1 Design rules of DDI process [23, 24]

Rule 1	$t_0 \geq 2 \times$ twall $\times 1.05$ (5%: Thickness reduction ratio caused by erosion t_0: Blank thickness, twall: Liner wall thickness
Rule 2	V_b (Blank volume) $= V_L$ (Liner volume)
Rule 3	Draw ratio in each drawing do not exceed LDR.
Rule 4	Draw ratio in 1st deep drawing process is smaller than 2.2.
Rule 5	Draw ratio in 2nd drawing process is smaller than 1.3 or 1.56 (1.3 × 1.2). If intermediate annealing takes place after the first draw, then the values are higher by 20% (1.56).
Rule 6	Draw ratio in 3rd drawing process is smaller than 1.2.
Rule 7	Limit reduction ratio of cross-sectional area in ironing process (LRA ironing) is 35%.
Rule 8	When ironing processes are carried out two times in one stage, each reduction ratio of the cross-sectional area (RA ironing) should be the same.
Rule 9	Limit reduction ratio of the cross-sectional area (LRA) in each stage is 50%.

Park *et al. Chinese Journal of Mechanical Engineering* (2022) 35:15

Page 4 of 12

rules of the DDI process used in the actual field [23, 24]. The volume of the CNG pressure vessel liner shown in Figure 5 is 10014808 mm³, and the blank thickness and diameter are determined according to rules 1–2. The punch diameters and the dies in the 1ˢᵗ–3ʳᵈ stages are calculated by rules 3–9, where $d_{p(m)}$ and $d_{i(m\text{-}n)}$ are the punch diameters and inflow diameter of the workpiece in the mth stage and n^{th} process.

2.2 Definition of Tractrix Curve

A tractrix is a curve along which a point (P) moves under the influence of friction when pulled on a vertical line (*y*) by a line segment attached to a tractor point (Q). The point moves at a right angle to the initial line between the object and the puller at a constant speed, as shown in Figure 6. A tractrix curve is defined by parameter *t* and shape coefficient S_c, as shown in Eq. (1) and Eq. (2).

$$x = S_c(1 - \mathrm{sech}(t)), \tag{1}$$

$$y = -S_c(t - \tanh(t)). \tag{2}$$

2.3 Calculation Method to Design Tractrix Curve

In the conventional design method for a tractrix curve, the shape coefficient (S_c) is calculated by Eq. (3) using the blank diameter (D_0) and inflow diameter of the workpiece (d_i). The tractrix curve is then obtained by Eqs. (1), (2), as shown in Figure 7.

$$S_c = \frac{D_0 - d_i}{2}. \tag{3}$$

Eq. (4) shows the slope of the tangent line at a point on the tractrix curve and is found by differentiating Eqs. (1) and (2) with respect to parameter *t*. It can then be rewritten as Eq. (5). From Eqs. (4) and (5), parameter *t* is expressed as the inflow angle of the material (θ), as shown in Eq. (6).
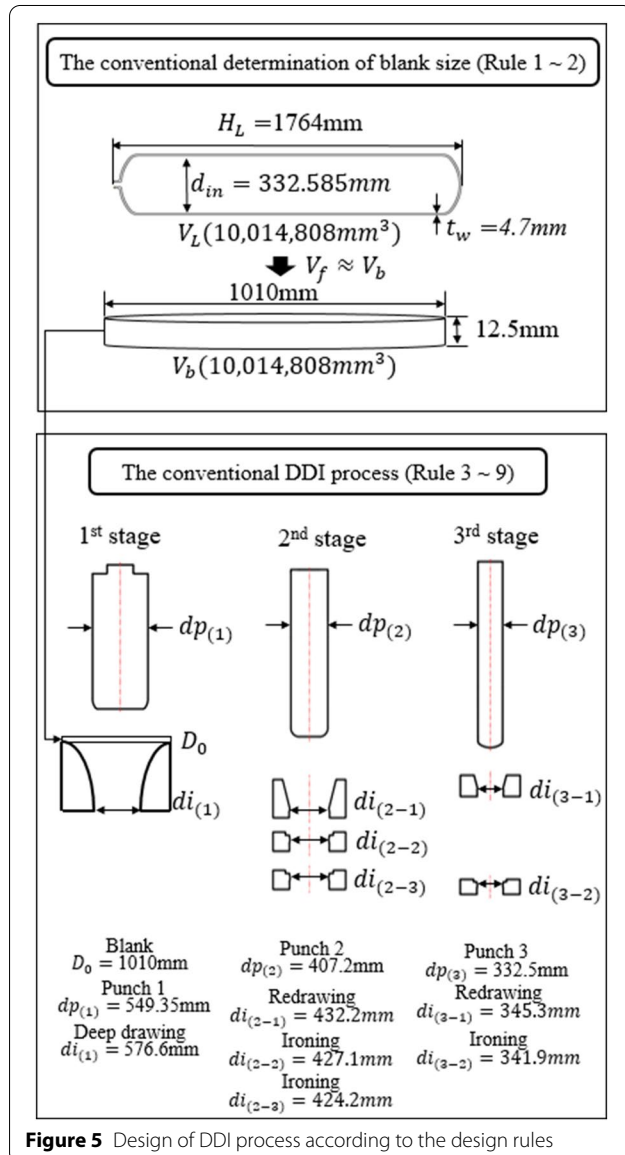

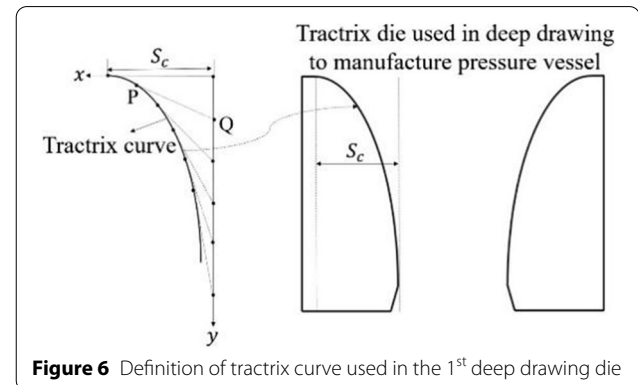**Figure 5** Design of DDI process according to the design rules

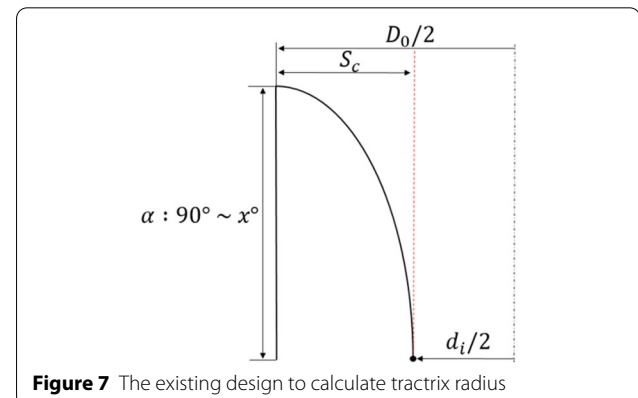**Figure 6** Definition of tractrix curve used in the 1ˢᵗ deep drawing die

Figure 7 The existing design to calculate tractrix radius

$$\frac{dy}{dx} = -\sinh(t), \tag{4}$$

$$\frac{y}{x} = \tan(90 - \theta), \tag{5}$$

$$t = \sinh^{-1}(\tan(90 - \theta)). \tag{6}$$

Eq. (7) is obtained by substituting Eq. (6) into Eq. (1), and the length of the tractrix curve in the *x*-direction is defined as the difference between the blank diameter (D_0) and the inflow diameter of the workpiece (d_i), as shown in Eq. (8). Therefore, by substituting Eq. (8) into Eq. (7), Eq. (9) is expressed to calculate the shape coefficient (S_c), as illustrated in Figure 8.

$$x = S_c - S_c \cdot \text{sech}(-\sinh^{-1}(\tan(90 - \theta))), \tag{7}$$

$$x = \frac{D_0}{2} - \frac{d_i}{2}, \tag{8}$$

$$S_c = \frac{D_0 - d_i}{2[1 - \text{sech}\left(-\sinh^{-1}(\tan(90 - \theta))\right)]}. \tag{9}$$

Eq. (9) can design variable shapes of a tractrix die within the limit of the draw ratio with D_0 (blank diameter), d_i (inflow diameter), and θ (inflow angle). It suggests the optimal inflow angle with no forming defects (wrinkling, folding, fracture). Figure 9 shows the variation of the tractrix curve according to the shape coefficients (S_c) obtained from Eq. (9) when the 1st draw ratio (D_0/d_p) is given as 1.84, which is used in the existing process.

3 Design of Initial Blank to Prevent Forming Defects

The forming analyses of the 1st deep drawing process were conducted by varying the inflow angle of the workpiece to find out the onset and development of wrinkling and folding under different thicknesses using the

Figure 9 Variation of tractrix curves according to the shape coefficients (*Sc*) ($\boldsymbol{D_0}/\boldsymbol{D_p} = 1.84$)
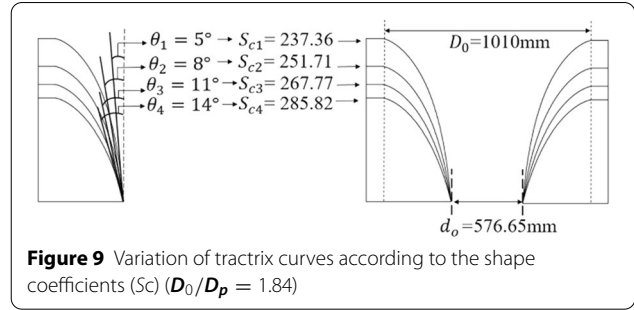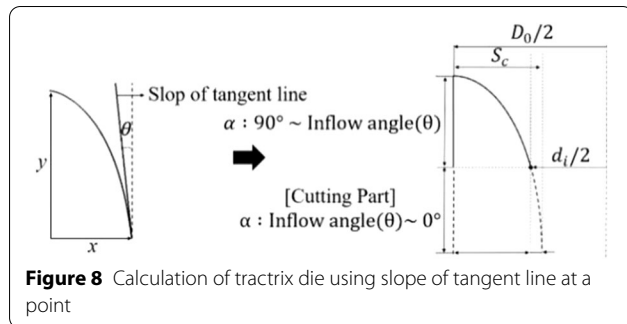
commercial software Forge NxT 2.0. The key factors affecting the wrinkling and folding are as follows.

- Friction and lubrication: The friction coefficient obtained by the friction test is 0.056, and its value is applied to the analysis of FEM. A Parkerizing process is also carried out for lubrication.
- Die shape: Die shape is controlled by the inflow angle (θ) obtained from Eq. (9) and has a large influence on preventing wrinkling and folding by reducing compressive stress in a deep drawing process without a blank holder.
- D_0/d_p, d_p/t_0: These are used to check the feasibility of the deep drawing with the tractrix die, and the first stage (deep drawing process) is carried out successfully to control inflow angles obtained from a variety of tractrix curves.

3.1 Analysis Model and Conditions

The analysis model consists of the tractrix die, punch, and blank, and its dimensions are a punch diameter (d_p) of 549.35 mm, inflow diameter of the workpiece (d_i) of 576.6 mm, initial blank thickness (t_0) of 12.5 mm, and blank diameter (D_0) of 1010 mm, as shown in Figure 10. The workpiece is set to a deformable domain with a volume mesh, which is periodically remeshed as the process progresses. Negligible deformation occurs in the die and
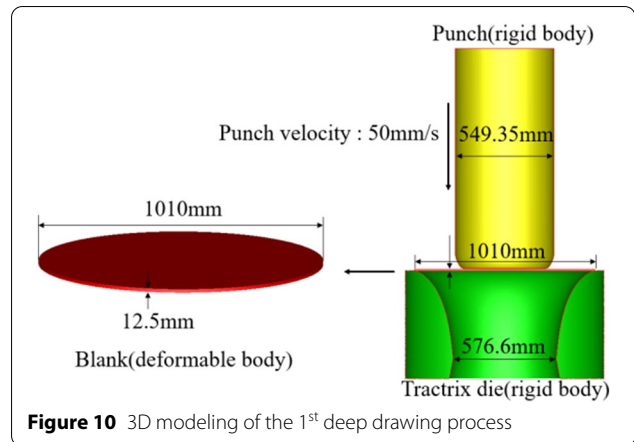

Figure 8 Calculation of tractrix die using slope of tangent line at a point

Figure 10 3D modeling of the 1st deep drawing process

Park *et al. Chinese Journal of Mechanical Engineering*   (2022) 35:15

Page 6 of 12

Table 2 Properties of material (34CrMo4)

Density (kg/m³)	Young's modulus (GPa)	Poisson's ratio
7850	200	0.3
Yield strength (MPa)	Ultimate strength (MPa)	
303.1	515.5	

Table 3 Coefficient of Hansel-Spittel equation in 34CrMo4

A	m_2	m_1, m_3 - m_9
887.02	0.213	0

Table 4 Blank diameter according to blank thickness (mm)

Blank diameter	Blank diameter	Inflow diameter
12	1031	576.6
11	1077	576.6
10	1129	576.6
9	1190	576.6
8	1262	576.6
7	1350	576.6

Table 5 Forming defects according to blank thickness and the inflow angles

Inflow angle Thickness	t_0: 7 mm D_0: 1350 mm	t_0: 8 mm D_0: 1263 mm	9–12 mm
1°	Folding	Folding	Non-defect
5°	Folding	Folding	Non-defect
6°	Folding	Folding	Non-defect
7°	Folding	Folding	Non-defect
8°	Folding	Wrinkling	Non-defect
9°	Folding	Wrinkling	Non-defect
10°	Folding	Wrinkling	Non-defect
11°	Folding	Wrinkling	Non-defect
12°	Folding	Wrinkling	Non-defect
13°	Folding	Wrinkling	Non-defect
14°	Folding	Wrinkling	Non-defect

Figure 11 Onset and decrease of wrinkling and folding in case of the inflow angle of 8)

the punch during the analysis, so they are assumed as rigid bodies with a surface mesh [25]. The punch velocity (50 mm/s) was suggested from the actual field, and the friction coefficient (μ) was defined as 0.056 [1].

The material properties and the flow stress equation used in FEA were obtained through a room-temperature tensile test of the liner material, 34CrMo4, as shown in Table 2 and Eq. (10). Forge NxT 2.0 software defined the flow stress using the Hansel-Spittel model [26, 27] shown in Eq. (11), which is based on a relation of the variables of strain, strain rate, and temperature. Therefore, the property coefficient of Eq. (11) should be derived using Eq. (10), as shown in Table 3 [28].

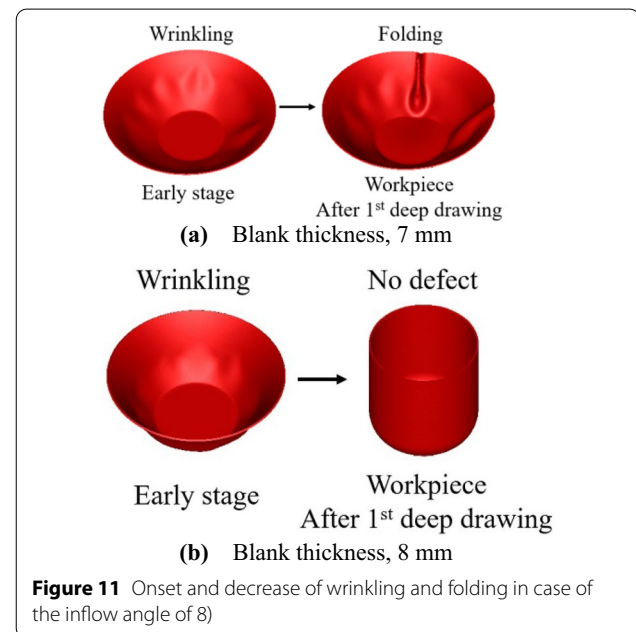$$\overline{\sigma} = 887.02\overline{\varepsilon}^{0.123}[\text{MPa}], \tag{10}$$

$$\overline{\sigma} = Ae^{m_1 T} T^{m_9} \varepsilon^{m_2} e^{\frac{m_4}{\varepsilon}} (1+\varepsilon)^{m_5 T} e^{m_7 \varepsilon} \dot{\varepsilon}^{m_3} \varepsilon^{m_8 T}. \tag{11}$$

3.2 Design of Initial Blank Thickness

Wrinkling and folding caused by compressive hoop stress in the deep drawing process are associated with the blank thickness and shape of the tractrix die. Therefore, an analysis was carried out by varying the blank thicknesses
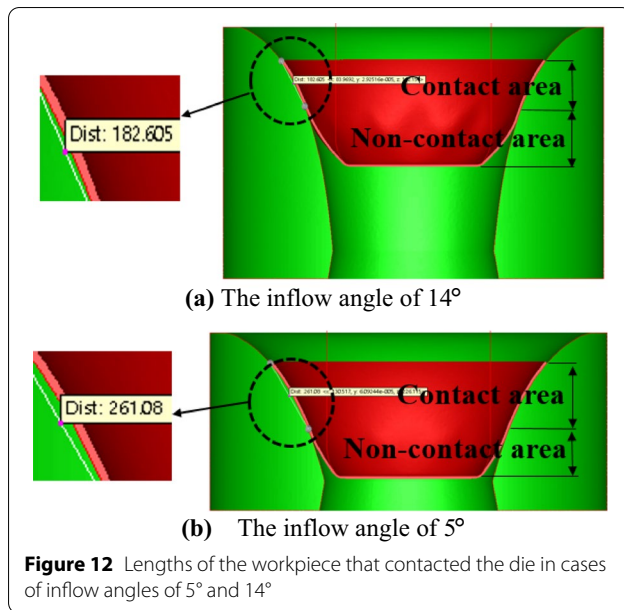
(7–12 mm), as shown in Table 4, and its results are expressed in Table 5.

The inflow angle of the workpiece was conducted up to 14°, in which the load corresponds to 832 t in the blank thickness (12 mm) when considering the rated load of the press (850 t). When the blank thickness was 7 mm, folding was observed at all inflow angles, as shown in Figure 11a, and when 8 mm, observed in the inflow angles below 7°. But when the angles were over 8°, the initial wrinkling decreased while the workpiece went through the die, as illustrated in Figure 11b.

(a) The inflow angle of 14°

(b) The inflow angle of 5°

Figure 12 Lengths of the workpiece that contacted the die in cases of inflow angles of 5° and 14°

During the deep drawing process, wrinkling can be removed at the end of the punch's stroke, as shown in Figure 12b, which causes deterioration of the formability and uneven distribution of the thickness along the drawing direction [23].

In order to verify the effect of the inflow angles on forming defects, lengths of the workpiece that contacted the die were compared at different inflow angles (5° and 14°), blank thickness (8 mm), and punch strokes (450 mm). The contact length was 261 mm at the inflow angle of 14° and was longer than that at 5° (183 mm). The results are shown in Figure 12. The contact length was longer with the increase of the inflow angles, and then friction resistance was greater, so the wrinkling was decreased.

Among the blank thicknesses (9–12 mm) not to occur wrinkling and folding determined, the initial minimum blank thickness (10 mm) was determined according to design rule (1) $[t_0(4.7\ mm) \geq 2 \times t_{wall} \times 1.05]$ in Table 1 while considering the design specification of the bottom part and corrosion in heat treatment. The blank diameter (D_0) was calculated to be 1129 mm from the constant volume (10014808 mm^3), and the draw ratio (D_0/d_p) should be within the LDR (2.2) in design rule (4).

4 The New Design of 1st Deep Drawing Process

Forming analyses according to the inflow angles (5°–14°) were conducted on the blank diameter (1129 mm), blank thickness (10 mm), inflow diameter of the workpiece (576.6 mm), and the maximum forming loads obtained just before the workpiece passed through the inflow
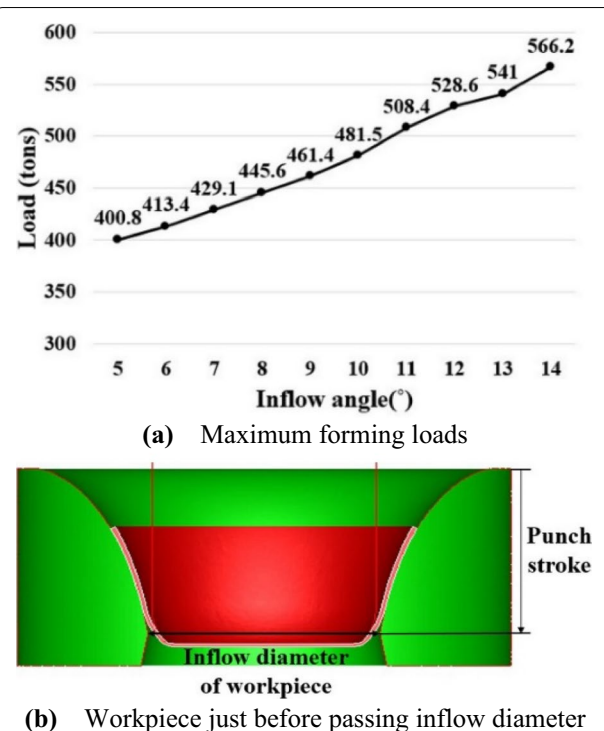

(a)　Maximum forming loads

(b)　Workpiece just before passing inflow diameter

Figure 13 Maximum forming loads according to the inflow angle (5°–14°)

diameter of the workpiece, as shown in Figure 13. The tractrix die prevents wrinkling and folding by increasing the inflow angle of the workpiece, but it causes the forming load to increase, as shown in Figure 13, and then it leads to fracture of the workpiece.

4.1 Prediction of Fracture

The 1st deep drawing should be conducted within the LDR to avoid fracture caused by the radial stress (σ_r) of Eq. (12), as shown in Figure 14 [29, 30]. The radial stress (σ_r), friction coefficient (f) between the blank and die,

Figure 14 Scheme of radial stress occurring in the workpiece during the 1st deep drawing
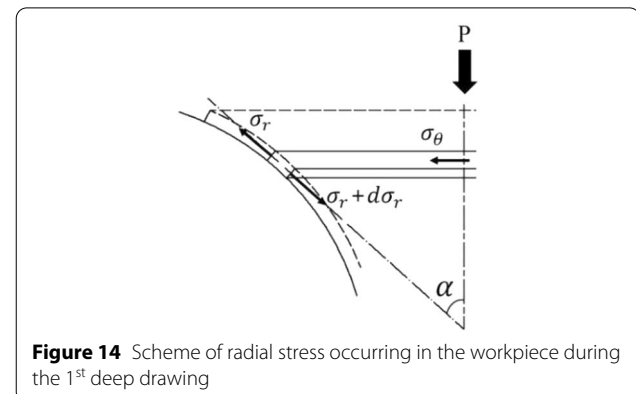
angle of the tractrix die (α), radius of the tractrix die (r), and strength (σ_Y) are expressed in Eq. (13) by the Tresca yield criterion.

$$\frac{\mathrm{d}\sigma_r}{\mathrm{d}r} + f \cdot \left(\frac{\mathrm{d}\alpha}{\mathrm{d}r} - \frac{\cot\alpha}{r} \right) \cdot \sigma_r = -(1 + f \cdot \cot\alpha) \cdot \frac{\sigma_Y}{r}, \tag{12}$$

$$\sigma_y = \sigma_r - \sigma_\theta. \tag{13}$$

The fracture in a deep drawing process occurs from high tensile stress caused by the punch's feeding direction and is judged by the relative radial stress ($\overline{\sigma}_r = \sigma_r / \sigma_Y$), so it is expected by Eq. (15), which is derived from Eq. (12)–Eq. (14).

$$\overline{\sigma}_r = \frac{\sigma_r}{\sigma_Y}, \tag{14}$$

$$\frac{\mathrm{d}\overline{\sigma}_r}{\mathrm{d}r} + f \cdot \left(\frac{\mathrm{d}\alpha}{\mathrm{d}r} - \frac{\cot\alpha}{r} \right) \cdot \overline{\sigma}_r = -\frac{1 + f \cdot \cot\alpha}{r}. \tag{15}$$

The tractrix curve shown in Figure 15 is expressed with the tractrix radius (r), which is the distance from a point C on the tractrix curve to the central axis, as well as the tractrix angle (α) between the central axis and the slope of the tangent line at point C.

r and $\mathrm{d}r$ at point C can be expressed as Eqs. (16) and (17).

$$r = r_i + S_c \cdot \sin\alpha, \tag{16}$$

$$\mathrm{d}r = S_c \cdot \cos\alpha \cdot \mathrm{d}\alpha. \tag{17}$$

Eq. (18) is derived by substituting Eqs. (16) and (17) into Eq. (15), and Eq. (19) can be obtained by substituting the dimensionless constant K (r_i/a) into Eq. (18). $\overline{\sigma}_r$ at the tractrix angles (α) of 0° to 90° can be obtained by integration of Eq. (19), and $\overline{\sigma}_r \geq 1$ means that fracture occurs.

$$\frac{\mathrm{d}\overline{\sigma}_r}{\mathrm{d}\alpha} - f \cdot \left(S_c \cdot \cos\alpha \cdot \frac{\cot\alpha}{r_i + S_c \cdot \sin\alpha} - 1 \right) \cdot \overline{\sigma}_r$$
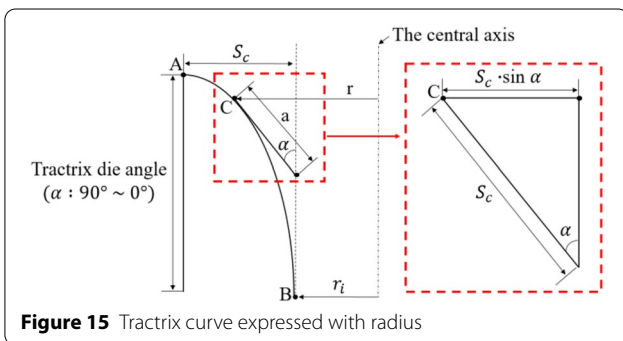$$= -S_c \cdot \cos\alpha \cdot \frac{1 + f \cdot \cot\alpha}{r_i + S_c \cdot \sin\alpha}, \tag{18}$$

$$\frac{\mathrm{d}\overline{\sigma}_r}{\mathrm{d}\alpha} - f \cdot \left(\cos\alpha \cdot \frac{\cot\alpha}{K + \sin\alpha} - 1 \right) \cdot \overline{\sigma}_r$$
$$= -\cos\alpha \cdot \frac{1 + f \cdot \cot\alpha}{K + \sin\alpha}. \tag{19}$$

The shape of the tractrix die using Eq. (9) is shown in Figure 16 and has a gap of $S_c \cdot \mathrm{sech}(t)$ in relation to the tractrix radius compared to the conventional shape shown in Figure 7. The tractrix radius is represented by Eq. (20), and Eq. (19) can be rewritten as Eq. (21) by substituting Eq. (20) and Eq. (17) into Eq. (15).

$$r = r_i + S_c \cdot \sin\alpha - S_c \cdot \mathrm{sech}(t), \tag{20}$$

$$\frac{\mathrm{d}\overline{\sigma}_r}{\mathrm{d}\alpha} - f \cdot \left(\cos\alpha \cdot \frac{\cot\alpha}{K \cdot (1 - \mathrm{sech}(t)) + \sin\alpha - \mathrm{sech}(t)} - 1 \right) \cdot \overline{\sigma}_r$$
$$= -\cos\alpha \cdot \frac{1 + f \cdot \cot\alpha}{K \cdot (1 - \mathrm{sech}(t)) + \sin\alpha - \mathrm{sech}(t)}. \tag{21}$$

The constant $K \cdot (1 - \mathrm{sech}(t)) - \mathrm{sech}(t)$ in Eq. (21) is defined by K' in Eq. (22), and Eq. (21) is expressed as Eq. (23). Fracture in the tractrix die can be predicted by integration of Eq. (23).

$$K' = K \cdot (1 - \mathrm{sech}(t)) - \mathrm{sech}(t), \tag{22}$$

$$\frac{\mathrm{d}\overline{\sigma}_r}{\mathrm{d}\alpha} - f \cdot \left(\cos\alpha \cdot \frac{\cot\alpha}{K' + \sin\alpha} - 1 \right) \cdot \overline{\sigma}_r$$
$$= -\cos\alpha \cdot \frac{1 + f \cdot \cot\alpha}{K' + \sin\alpha}. \tag{23}$$

Figure 15 Tractrix curve expressed with radius
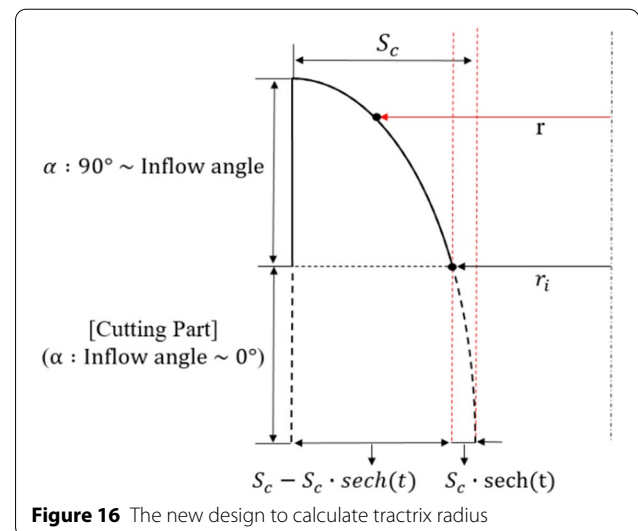

Figure 16 The new design to calculate tractrix radius

Table 6 Relative radial stress according draw ratios (2.3–2.6) and inflow angles (1°–10°)

Draw ratio (2.3)										
Inflow angle of workpiece (°)	1	2	3	4	5	6	7	8	9	10
Relative radial stress	0.89	0.89	0.90	0.90	0.91	0.92	0.93	0.94	0.95	0.96
Draw ratio (2.4)										
Inflow angle of workpiece (°)	1	2	3	4	5	6	7	8	9	10
Relative radial stress	0.93	0.93	0.94	0.94	0.95	0.96	0.97	0.98	0.99	1.00
Draw ratio (2.5)										
Inflow angle of workpiece (°)	1	2	3	4	5	6	7	8	9	10
Relative radial stress	0.96	0.97	0.98	0.98	0.99	1.00	1.01	1.02	1.03	1.04
Draw ratio (2.6)										
Inflow angle of workpiece (°)	1	2	3	4	5	6	7	8	9	10
Relative radial stress	1.00	1.00	1.01	1.02	1.03	1.04	1.05	1.06	1.07	1.08

Table 7 Comparison of results according to draw ratios (2.3–2.5) in the 1st deep drawing

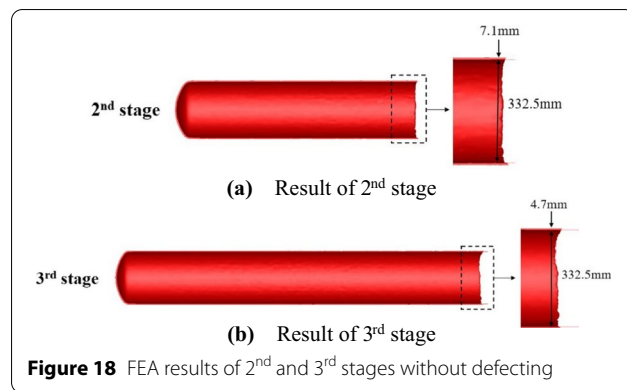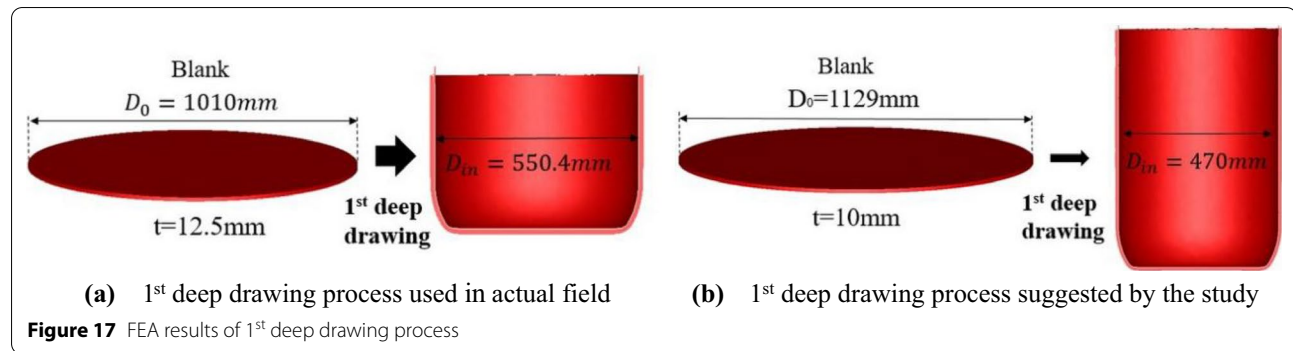| Draw ratio		2.3	2.4	2.5
DDI process	1st stage	Deep drawing	Deep drawing	Deep drawing
	2nd stage	Redrawing 1 → ironing 1 → ironing 2	Redrawing → ironing 1	Redrawing → ironing 1
	3rd stage	Redrawing 2 → ironing 3	Ironing 2	Ironing 2
Number of processes		5	4	4
Inflow angle of workpiece		13°	9°	5°
Volume of tractrix die		4.66×10^8 mm^3	5.71×10^8 mm^3	7.45×10^8 mm^3

4.2 New Design of Tractrix Die

According to rule (4) in Table 1, a drawing process was carried out under a draw ratio of 2.2, which is used in the actual field. Now, reduction of the number of operations is possible due to the improved draw ratio. When the draw ratio was 2.3, a defect was not found at all inflow angles, when the 2.4 and 2.5, not observed under 9° and under 5°, respectively, but when 2.6, observed at all inflow angles. Therefore, the inflow angle should be
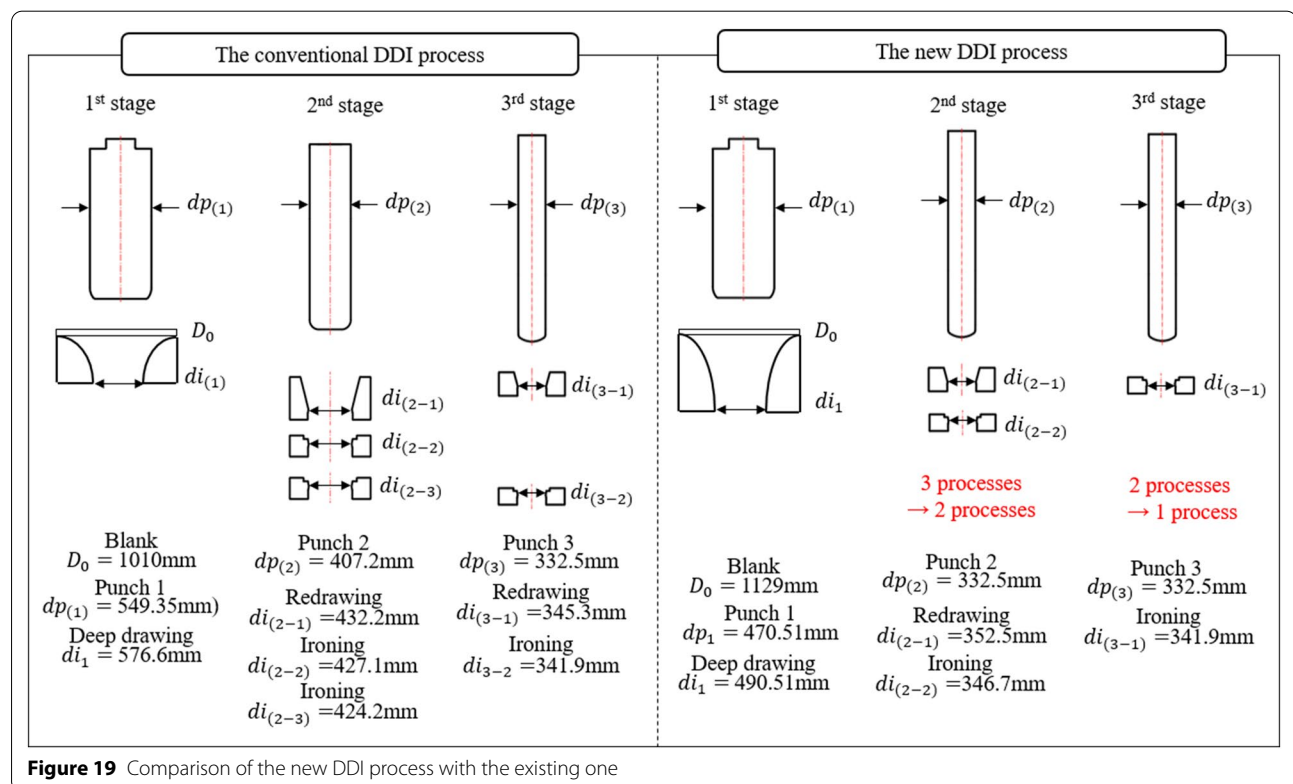
Table 8 Design of punch and die according to the best draw ratio (2.4) and inflow angle (9°)

Stage		Dimension of die	Draw ratio and reduction ratio of cross-sectional area
1st stage	Deep drawing	$D_0 = 1{,}129$ mm $dp_1 = 470.51$ mm $di_1 = 490.51$ mm	$D_0/dp_1 = 2.4$ $A_1 = \frac{\pi}{4}\left(di_1{}^2 - dp_1{}^2\right) = 15{,}095.7$ mm^2
2nd stage	Redrawing	$dp_2 = 332.5$ mm $di_{2-1} = 352.5$ mm	$d_{p1}/d_{p2} = 1.42$ $A_{21} = \frac{\pi}{4}\left(di_{2-1}{}^2 - dp_2{}^2\right) = 10{,}760$ mm^2
	Ironing 1	$di_{2-2} = 346.7$ mm	$A_{22} = \frac{\pi}{4}\left(di_{2-2}{}^2 - dp_2{}^2\right) = 7{,}574.9$ mm^2 $RA_{Ironing,22} = 1 - \frac{A_{2-2}}{A_{2-1}} = 29.6\%\ (< 35\%)$ $RA_{total,2} = 1 - \frac{A_{2-2}}{A_1} = 49.8\%\ (< 50\%)$
3rd stage	Ironing 2	$dp_3 = 332.5$ mm $di_{3-1} = 341.9$ mm	$A_{31} = \frac{\pi}{4}\left(di_{3-1}{}^2 - dp_3{}^2\right) = 4{,}979$ mm^2 $RA_{Ironing,3-2} = 1 - \frac{A_{3-1}}{A_{2-2}} = 34.3\%\ (< 35\%)$ $RA_{total,3} = 1 - \frac{A_{31}}{A_{22}} = 34.3\%\ (< 50\%)$

Figure 17 FEA results of 1st deep drawing process

(a)   1st deep drawing process used in actual field

(b)   1st deep drawing process suggested by the study

(a)   Result of 2nd stage

(b)   Result of 3rd stage

Figure 18 FEA results of 2nd and 3rd stages without defecting

decreased in order to avoid forming defects due to the radial stress when the draw ratio increases. In cases of the draw ratios of 2.3, 2.4 and 2.5, the inflow angles are 13°, 9°, and 5°, respectively. Their DDI process design results are shown in Table 6.

Ironing process 2 in the 2nd stage and redrawing process 1 in the 3rd stage were removed when the draw ratio were 2.4 and 2.5. From Table 7, compared the draw ratio (2.5) and the inflow angle (5°) to the draw ratio (2.4) and the inflow angle (9°), the latter was chosen to have the minimum volume of the tractrix die, which has low manufacturing cost without forming

Figure 19 Comparison of the new DDI process with the existing one

Park *et al. Chinese Journal of Mechanical Engineering*   (2022) 35:15

Page 11 of 12

defects. The punch and die dimensions according to the design rules are shown in Table 8.

4.3 Verification of the 1st Deep Drawing Process suggested

Forming simulations with punch and die dimensions suggested in Table 8 were conducted, and forming defects did not occur, as shown in Figures 17 and 18. The new DDI process (draw ratio: 2.4, blank thickness: 10 mm, inner diameter of the workpiece: 491 mm) lets us remove the ironing process in the 2nd stage and redrawing process in the 3rd stage, as shown in Figure 19, unlike the existing process (draw ratio: 1.84 used in actual field, blank thickness: 12.5 mm, inner diameter of the workpiece: 550.4 mm). Therefore, improvement of the productivity and reduction of the production cost were possible.

5 Conclusions

This study has conducted the 1st deep drawing process to manufacture a CNG high-pressure vessel (Type II) and has developed a theoretical approach to generate a tractrix curve and, according to it, predicted fracture of the workpiece. Also, effects of the thickness and inflow angle of the workpiece on forming defects (wrinkling and folding) were investigated through FEA. The summaries are as follows.

1) Effects of the thickness and inflow angle of the workpiece on wrinkling and folding were investigated through shapes of the tractrix die, which were calculated by using the initial blank thickness (t_0), inflow diameter of the workpiece (d_i), and inflow angle of the workpiece (θ) and were verified through FEA.

2) The contact length was longer with the increase of the inflow angles, and then friction resistance was greater, so the wrinkling was decreased.

3) A theoretical approach to predict fracture was proposed using the relative radial stress equation, and based on its result, the best draw ratio and inflow angle without fracture were determined as 2.4 and 9°, respectively.

4) Compared to the conventional 1st deep drawing process, the new DDI process obtained from the study (draw ratio: 1.84 → 2.4, blank thickness: 12.5 mm → 10 mm, inner diameter of the workpiece: 549.35 mm → 491 mm) lets us remove ironing 2 process in the 2nd stage and the redrawing process in the 3rd stage, which contributes to improvement of the productivity and reduction of the production cost. The results of the study could be widely adopted to manufacture pressure vessels for various size and uses.

Authors' Information
Gun-Young Park was born in 1986 and is in the doctor's course in the School of Mechanical Engineering, Pusan National University, Pusan, Korea. He received a master's degree in mechanical convergence technology from *Pusan National University, Korea*, in 2018. His major research fields are metal forming, finite element analysis, and design of a pressure vessel.
Hyo-Seo Kwak was born in 1989 and received an M.S. degree in School of Creative Engineering and a Ph.D. degree in mechanical convergence technology from *Pusan National University, Korea*, in 2012, 2014, and 2017. She is currently an assistant professor in *Dong-eui University, Korea*. Her research fields extend into machine design and FEM simulation.
Hyo-Seong Jang was born in 1990 and is in the doctor's course at *School of Mechanical Engineering, Pusan National University, Pusan, Korea*. He received a master's degree in creative engineering systems from *Pusan National University, Korea*, in 2015. His major research fields are gear design and computational fluid dynamics.
Chul Kim was born in 1961 and is a professor of mechanical engineering at *Pusan National University, Korea*. He received a doctoral degree in mechanical engineering from *Pusan National University, Korea*, in 1994. His major research fields are FEM simulation (structure, dynamic, and fluid analysis), optimal structural design, and high pressure vessels.

Author Details
[1]School of Mechanical Engineering, Pusan National University, Pusan 46241, South Korea. [2]Department of Mechanical Engineering, Dong-eui University, Pusan 47340, Korea.

References
[1] H S Kwak, G Y Park, H S Seong, et al. Integrated design of d.d.i., filament winding and curing processes for manufacturing the high pressure vessel (Type II). *Chinese Journal of Mechanical Engineering*, 2019, 32: 83. https://doi.org/10.1186/s10033-019-0396-9

[2] H S Kwak, G Y Park. Design of compressed natural gas pressure vessel (Type II) to improve storage efficiency and structural reliability. *Journal of Pressure Vessel Technology*, 2020, 142(1): 011303. https://doi.org/10.1115/1.4045027

[3] Y Abe, T Fujita, K Mori, et al. Improvement of formability in ironingironing of stainless steel drawn cups using low friction cermet dies. *Procedia Engineering*, 2014, 81: 1896-1901. https://doi.org/10.1016/j.proeng.2014.10.253

Park *et al. Chinese Journal of Mechanical Engineering* (2022) 35:15

Page 12 of 12

[4] M Khodsetan, G Faraji, K Abrinia. A novel ironing process with extra high thickness reduction: constrained ironing. *Materials and Manufacturing Processes*, 2015, 30: 1324-1328. https://doi.org/10.1080/10426914.2015.1037898

[5] J H Bae, H W Lee, C Kim. A study on integrated design for manufacturing processes of a compressed natural gas composite vessel. *International Journal of Precision Engineering and Manufacturing*, 2014, 15(7): 1311-1321. https://doi.org/10.1007/s12541-014-0471-1

[6] J B Nam, K S Han. Finite element analysis of deep drawing and ironing process in the steel D&I canmaking. *The Iron and Steel Institute of Japan International*, 2000, 40(12): 1223-1229. https://doi.org/10.2355/isijinternational.40.1223

[7] G O Lee, G Y Park, H S Kwak, et al. Forming of dome and inlet parts of a high pressure CNG vessel by the hot spinning process. *Trans. Korean Soc. Mech. Eng. A*, 2016, 40(10): 887- 894. https://doi.org/10.3795/KSME-A.2016.40.10.887

[8] S T Atul, M C L Babu. A review on effect of thinning, wrinkling and springback on deep drawing process. *Proceedings of the Institution of Mechanical Engineers, Park B: Journal of Engineering Manufacture*, 2019, 233(4): 1011-1036. https://doi.org/10.1177/0954405417752509

[9] K Bandyopadhyay, S K Panda, P Saha, et al. Limiting drawing ratio and deep drawing behavior of dual phase steel tailor welded blanks : FE simulation and experimental validation. *Journal of Materials Processing Technology*, 2015, 217: 48-64. https://doi.org/10.1016/j.jmatprote.2014.10.022

[10] G Angasu, K S Reddy. Deep drawing process parameters: A review. *International Journal of Current Engineering and Technology*, 2016, 6(4):1204-1215. https://doi.org/10.14741/ljcet/22774106/6.4.2016.20

[11] A R Joshi, K D Kothari, R L Jhala. Effects of different parameters on deep drawing process: review. *International Journal of Engineering Research and Technology*, 2013, 2(3): 1-5.

[12] R T Nirav. Effects of various parameters in deep drawing process over sheet metal to get optimum result. *International Journal of Engineering Development and Research*, 2014, 2(4): 2321-9939.

[13] R Narayanasamy, C Loganathan, J Satheesh. Some study on wrinkling behaviour of commercially pure aluminium sheet metals of different grades when drawn through conical and tractrix dies. *Materials and Design*, 2008, 29:1654-1665. https://doi.org/10.1016/j.matdes.2006.12.007

[14] R Narayanasamy, C Loganathan. Some studies on wrinkling limit of commercially pure aluminium sheet metals of different grades when drawn through Conical and Tractrix dies. *International Journal of Mechanics and Materials in Design*, 2006, 3: 129-144. https://doi.org/10.1007/s10999-006-9018-7

[15] N Kaneriya, D Shah, R Rana, et al. Effect of different parameters on deep drawing process for minimum stress and defects by experimental and simulation study : A review. *International Journal of Advance Engineering and Research Development*, 2016, 3(10).

[16] R Kesharwani, S Basak, S Panda, et al. Improvement in limiting drawing ratio of aluminum tailored friction stir welded balnks using modified conical tractrix die. *Journal of Manufacturing Processes*, 2017, 28: 137-155. https://doi.org/10.1016/j.jmapro.2017.06.002

[17] R K Kesharwani, S K Panda, S K Pal. Experimental investigations on formability of aluminum tailor friction stir welded blanks in deep drawing process. *Journal of Materials Engineering and Performance*, 2015, 24(2): 1038-1049. https://doi.org/10.1007/s11665-014-1361-5

[18] J P G Magrinho, C M A Silva, M B Silva, et al. Formability limits by wrinkling in sheet metal forming. *Proceedings of the Institution of Mechanical Engineers, Part L: Journal of Materials: Design and Applications*, 2018, 232(8): 681-692. https://doi.org/10.1177/1464420716642794

[19] R Narayanasamy, C Sathiya. Wrinkling behaviour of interstitial free steel sheets when drawn through tapered dies. *Materials & Design*, 2007, 28: 254-259. https://doi.org/10.1016/j.matdes.2005.07.005

[20] A Abdullah, M Emad, S Soliman, et al. Development of deep drawing without blank-holder for producing elliptic brass cups through conical dies. *Journal of Engineering Sciences*, 2013, 41(4): 1530-1548.

[21] A Abdullah, M Emad, S Soliman, et al. Finite element modeling and experimental results of brass elliptic cups using a new deep drawing process through conical dies. *Journal of Materials Processing Technology*, 2014, 214(4): 828-838. https://doi.org/10.1016/j.jmatprotec.2013.11.025

[22] L M A Hezam, M A Hassan, I M Hassab, et al. Development of a new process for producing deep square cups through conical dies. *International Journal of Machine Tolls & Manufacture*, 2009, 49: 773-780. https://doi.org/10.1016/j.ijmachtools.2009.04.001

[23] C H Kim, J H Park, C Kim, et al. Expert system for process planning of pressure vessel fabrication by deep drawing and ironing. *Journal of Materials Processing Technology*, 2004, 155: 1465-1473. https://doi.org/10.1016/j.jmatprotec.2004.04.350

[24] Heinz Tschaetsch. *Metal forming practise*. New York: Springer-verlag, 2006.

[25] F F Luis, S Lirio. Effect of surface roughness and lubrication on the friction coefficient in deep drawing processes of aluminum alloy aa1100 with fem analysis. *Revista Material*, 2019, 24, (3). https://doi.org/10.12776/ams.v21i4.642

[26] O Liang, X Liu, P Li, et al. Development and application of high-temperature constitutive model of HNi55-7-4-2 alloy. *Metals*, 2020, 10(9): 1250. https://doi.org/10.3390/met10091250

[27] X Chen, N Wang, X Ma, et al. Hot deformation behavior and Hansel-Spittel constitutive model of Cr5 alloy for heavy backup roll. *International Journal of Computational Materials Science and Surface Engineering*. 2018, 7: 205-217. https://doi.org/10.1504/IJCMSSE.2018.095321

[28] G Y Park, R K Park, H S Kwak, et al. Design of a combined redrawing-ironing process to manufacture a CNG pressure vessel liner. *Applied Sciences*. 2021, 11: 8295. https://doi.org/10.3390/app11188295

[29] P Rudolf, B Igor, K Jozef, et al. Evaluation of limiting drawing ratio (LDR) in deep drawing process. *Acta Metallurgica Slovaca*, 2015, 21(4): 258-268. https://doi.org/10.12776/ams.v21i4.642

[30] A Fazli, B Arezoo. An analytical method for prediction of limiting drawing ratio for redrawing stages of axisymmetric deep drawn components. *Journal of Manufacturing Science and Engineering*, 2014, 136(2). https://doi.org/10.1115/1.4026125